Desalination and Water Treatment
www.deswater.com
1944-3994/1944-3986 © 2013 Desalination Publications. All rights reserved
doi: 10.1080/19443994.2012.694202
51 (2013) 936–943
January
Taylor & Francis
Taylor & Francis Group

Amorphous aluminosilicate scaling characterization in a reverse osmosis membrane

S. Salvador Cob[a,*], C. Beaupin[a], B. Hofs[a], M.M. Nederlof[a], D.J.H. Harmsen[a], E.R. Cornelissen[a], A. Zwijnenburg[b], F.E. Genceli Güner[c], G.J. Witkamp[c]

[a]*KWR Watercycle Research Institute, Nieuwegein 1072, 3430 BB, The Netherlands*
Tel. +31(0)306069581; email: sara.salvador.cob@kwrwater.nl
[b]*Wetsus, Centre for Sustainable Water Technology, P.O. Box 113, Leeuwarden 8900 CC, The Netherlands*
[c]*Process & Energy Department, Delft University of Technology, Leeghwaterstraat 44, Delft 2628 CA, The Netherlands*

Received 14 March 2012; Accepted 10 May 2012

ABSTRACT

This paper describes the results of experiments performed in a high-recovery system to elucidate the silica scaling phenomenon and characterize the scaling. In this research, cation exchange pretreatment is used to reduce Ca^{2+}, Ba^{2+}, and Mg^{2+} levels to prevent scaling during subsequent nanofiltration (NF) and reverse osmosis (RO) filtration, in which RO is fed with NF concentrate. In a pilot plant, a series of experiments were carried out at a total (NF + RO) recovery of 91, 94, 96 and 98% with locally available tap water as feed water. Autopsy studies were performed with the RO membranes after each experiment. The fouling layer was studied using SEM-EDX, ATR-FTIR and fouling extraction to determine the structure and the composition of the fouling deposits. A thin dense fouling layer was observed, which covered approximately half of the membrane surface, after operating for 20 days at 91 and 94% recovery. At 96 and 98% recovery, the fouling layer was thicker and completely covered the membrane surface. The scaling layer was mainly composed of Si, Al, Fe and O. The amount of Si increased with increasing recovery. To work at these high recoveries for an extended period, further measures need to be taken to prevent silica scaling.

Keywords: Concentrate; Membrane fouling; Silica scaling; Colloidal fouling; Concentration polarization

1. Introduction

Silica scaling is one of the main issues in brackish water desalination where high recoveries are reached. The presence of silica in all kind of natural water complicates desalination processes owing to its high scaling potential [1–3]. The intricate chemistry of silica enhances the complexity of this problem. It is important to gain further insight in the way silica scales the membranes to prevent it.

To work at high recoveries in nanofiltration (NF) and reverse osmosis (RO) membranes, the scaling salts must be removed in the pretreatment steps. This is rather easy for bivalent ions, such as Ca^{2+} and Mg^{2+},

*Corresponding author.

Presented at the International Conference on Desalination for the Environment, Clean Water and Energy, European Desalination Society, 23–26 April 2012, Barcelona, Spain

which can be removed by using a cation exchange resin. When the bivalent cations are removed before membrane treatment, silica can become the limiting factor in RO, especially at high recoveries. Silica can be removed by an anion exchange resin, but unfortunately the affinity of silica for these resins is very low. The removal of silica is crucial to reach high recoveries, and further investigations are needed. Silica has a low solubility of about 117 ppm in water at pH 7 and at 25˚C. When its solubility limit is exceeded in the absence of a suitable crystallization surface on which the soluble silica might be deposited, the monomer polymerizes by condensation of the silanol groups [4].

In a previous work, we investigated the feasibility of achieving a high total recovery (91–98%) in a system composed of a cation exchange (CIEX) resin, followed by an NF membrane and an RO membrane, which treats the NF concentrate [5]. The feed water is tap water, which is produced from ground water pretreated by aeration and rapid sand filtration. We found that the cation exchange unit removes most (>99%) of the bivalent cations, thereby preventing the deposition of sparingly soluble salts in the RO membrane. The CIEX is followed by a feed and bleed NF unit at a recovery of 75–90%. Subsequently, the concentrate stream is fed to a feed and bleed RO unit at a recovery of 75–90%. For the NF + RO system, this leads to a NF + RO recovery of 91–99%. In practice, the total recovery of the system including CIEX is about 1% lower than the recovery reached with the two membrane stages, as a result of water losses due to regeneration of the CIEX.

In this research, the main objective is to investigate the layer of silica scaling on the RO membrane that is formed even after removing bivalent cations with CIEX prior to NF and RO at high recoveries of 91–98%. Previously, we have found that scaling takes place at these recoveries [5]; here, we present a more extensive analysis of the scaling of the RO membrane.

2. Materials and methods

2.1. Pilot plant

A pilot plant has been constructed at KWR Watercycle Research Institute to carry out silica scaling research at high-recovery RO (see Fig. 1). The pilot was described previously [5].

The membrane permeability, normalized pressure drop (NPD) (feed-concentrate) and salt passage, based on electrical conductivity (EC) measurements, were monitored for both membranes to investigate the beginning of scaling and other types of fouling.

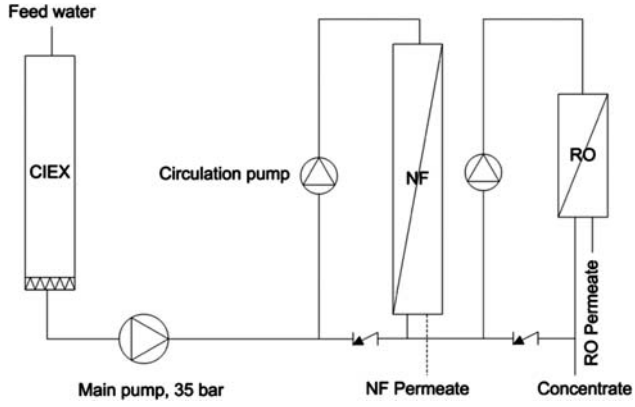

Fig. 1. Scheme of the pilot plant used in this research.

2.2. Water analysis

The different water streams (feed water, CIEX treated (feed) water, the NF feed, NF permeate, NF concentrate, RO feed, RO permeate and RO concentrate) were analyzed to determine the concentration of inorganic compounds including the scaling salts and calculate the rejection behavior of the membranes. With these analyses the mass balance within the system was calculated.

Dissolved organic carbon (DOC) was analyzed in accordance with ISO 8245 and ISO 1484. Before preservation, the samples were filtered using a 0.45-μm membrane filter.

Most of the inorganic compounds present in the different streams were measured with ion couple plasma mass spectrometry (ICP-MS) (Elan 6000, from Perkin Elmer). These analyses were conducted by the Laboratory of Materials Research and Chemical Analyses of KWR.

Chloride and sulfate concentrations, however, were measured with an in-house method by Vitens Laboratorium B.V. (Leeuwarden, the Netherlands). HCO_3^- and CO_3^{2-} concentrations were measured by pH titration, according to the NEN 6531.

Also, the water after CIEX was monitored with a Ca^{2+} selective electrode (Thermo Scientific Orion 9700 BN WP) to determine the Ca^{2+} concentration of the feed water of the first circulation stage. The regeneration of the resin was done regularly based on these measurements and the need to prevent breakthrough of bivalent cations to the NF.

The feed water of the installation was locally available drinking water from groundwater treated at plant Tull en 't Waal (Water Supply Company Vitens) by aeration and rapid sand filtration with the addition of polyaluminum chloride and without post-chlorination. The quality of the water is given in Table 1. The water had an average temperature of 12˚C.

Table 1
Average quality of the feed water (all concentrations as mg/L except pH)

Ca	70
Na	14
Mg	5.86
Al	0.02
K	1.25
Fe	0.01
Ba	0.05
Cr	0.01
Cu	0.05
Sr	0.23
B	0.01
Cl	9.19
HCO_3	277
SO_4	<2
SiO_2	20
DOC	1.95
pH	8.12

2.3. Membrane autopsy

2.3.1. Membrane surface characterization

After each run, a membrane autopsy was performed of the RO membrane. A visual inspection of the two leafs of the membrane was first carried out followed by the collection of 3 representative samples of 3 × 3 cm^2 taken at different locations of the membrane (inlet, middle, outlet). The samples were analyzed using a JEOL-6480LV Scanning Electron Microscope (SEM) (JEOL Company) equipped with Noran System SIX X-ray microanalysis (EDX) system (Thermo Electron Corporation) to determine the structure and the composition of the fouling (scaling) layers. The samples were coated with a thin (10 nm) Au layer. An accelerating voltage of 6 kV was used for SEM observation and 10 kV for the EDX analysis.

Different techniques have been used to try to characterize qualitatively the scaling formed in the membranes, such as Raman spectroscopy (Horiba/Jobin Yvon, Labram HR L/2/719), powder X-ray diffraction (XRD) (Bruker D8 Advance) and infrared spectroscopy (ATR-FTIR) (Shimadzu 4800).

2.3.2. Extraction of silica from the fouled membranes

To quantify the amount of silica scaling attached to the membrane a method to dissolve the silica was developed. The solubility of silica is much higher at high pH; therefore, we used a concentrated NaOH solution to dissolve the layer of silica scaling [6,7]. Representative samples of 3 by 3 cm from each membrane were placed in plastic beakers with NaOH solution. Among the different pH and stirring times that were tested, pH 14 and three days were found to be the optimal conditions. At lower pH and/or shorter time, the layer was (probably) not completely dissolved, and at pH 14 and longer time the membranes were visually damaged. After three days, the pieces of membrane were removed and the solutions were analyzed by means of ICP-MS. A blank (dry clean membrane piece added) experiment was performed and used for correction. All experiments were performed in quadruplicates. The obtained values for the experiment at 98% recovery were multiplied by two to correct for the shorter run time of this experiment (11 days vs. 20 days for the other recoveries).

2.4. Concentration polarization

The concentration polarization factor (CP) has been calculated according to the classical film model [8]:

$$\mathrm{CP} = \exp\left(\frac{J_v}{k_m}\right) \tag{1}$$

where J_v is the flux and k_m the mass transfer coefficient.

However, this equation only holds when there is no fouling on the membrane surface, because fouling hinders the solute diffusion across the fouling layer.

We have estimated the CP factor for a fouled membrane according to Chong [9]:

$$\mathrm{CP} = \exp\left(\frac{J_v}{k_{eff}}\right) \tag{2}$$

with $\frac{1}{k_{eff}} = \frac{1}{k_m} + \frac{1}{k_f}$

Here, k_{eff} is the effective mass transfer coefficient that combines the mass transfer in an un-fouled membrane and the mass transfer, k_f, in a fouled membrane.

$$k_f = \frac{D_f}{\delta_f}$$

Where D_f is the solute diffusion in the cake layer and δ_f the cake layer thickness.

$$D_f = D\left(\frac{\varepsilon}{1 - \ln \varepsilon^2}\right)$$

Where ε is the porosity of the cake layer.

Table 2
Summary of the experiments performed in our system

Total recovery (%)	NF recovery (%)	RO recovery (%)	Feed flow (l/h)	Feed pressure (bar)	NF flux (l/m^2 h)	RO flux (l/m^{2}h)
90.9	69.4	70.2	65	10	17.26	19.94
93.8	76.1	74.3	69	11	18.24	17.80
96.3	78.2	83.3	88	17	23.75	21.30
98.2	89.0	83.2	122	17	38.98	16.90

3. Results

3.1. Silica scaling experiments at different recoveries

3.1.1. Operation parameters

Experiments were carried out with the pilot plant at different operational settings to achieve different total system recovery values (Table 2).

During the experiments, the EC passage, membrane permeability and NPD were monitored for both membranes, with a focus on the RO membrane, due to its high potential for scaling. All the experiments were carried out during 3 weeks, except the last experiment, which was stopped after 11 days, due to the higher decrease in the RO permeability.

During the four experiments, there was no significant increase in the NPD (smaller than 0.5 bar). Therefore, no blocking of the feed channel seemed to occur.

A decrease was observed in the salt passage and membrane permeability of the RO membranes at all the different recoveries during the four runs. The decrease in the membrane permeability was higher at 98% recovery. These results are reported elsewhere [5].

3.1.2. Membrane surface characterization

The SEM-EDX analysis performed on the four RO membranes after the experiments revealed varying amounts of scaling.

At 91 and 94% recovery, about half of the membrane was covered with a 1–2-μm-thin layer of scaling ([5] and Fig. 2), while at 96 and 98% the complete surface was covered with a 5– to 10-μm-thick layer ([5] and Fig. 3). In all cases, the composition of the scaling was composed of organic matter, silicon (increasing with recovery), aluminum, sodium and iron. EDX results are reported elsewhere [5]. However these results are just a qualitative indication, since the membrane itself is also detected by the EDX. The percentage of membrane detected increases with decreasing the recovery but is not exactly known; hence, it is hard to quantify the relative occurrence of the elements in the scaling layer at different recoveries.

To further characterize the scaling layer, ATR-FTIR was performed on the four fouled RO membranes and a virgin RO membrane (Fig. 4).

The ATR-FTIR spectra from the four different samples reveal the same peaks. Peak intensity is higher for the membranes at 96 and 98% due to a higher amount of scaling on the membrane. All spectra show a large peak at 1,015 cm^{-1}. It possibly belongs to amorphous SiO_2, which normally has a peak at around 1,100 cm^{-1} [10] or amorphous aluminosilicates, which present a large peak around 1,000 cm^{-1} [11,12]. The broad band between 2,800 and 3,600 cm^{-1} can be attributed to hydrogen-bond OH surface groups, physisorbed water and other surface species [13]. In the experiments carried outat 91 and 94% recovery,

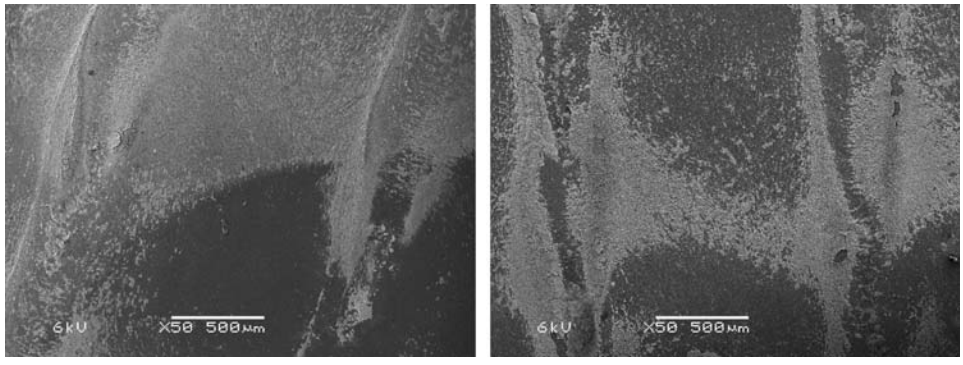

Fig. 2. SEM pictures of the RO membrane fouled at 91% total recovery (left) and 94% total recovery (right).

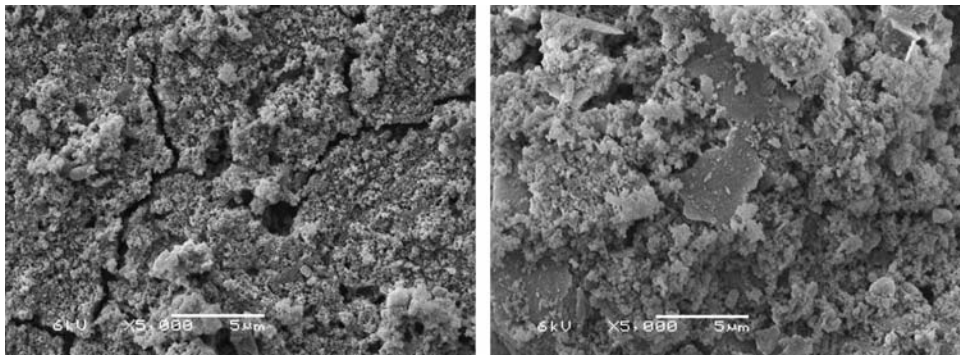

Fig. 3. SEM pictures of the RO membrane fouled at 96% total recovery (left) and 98% total recovery (right). Notice the different magnification compared with Fig. 2.

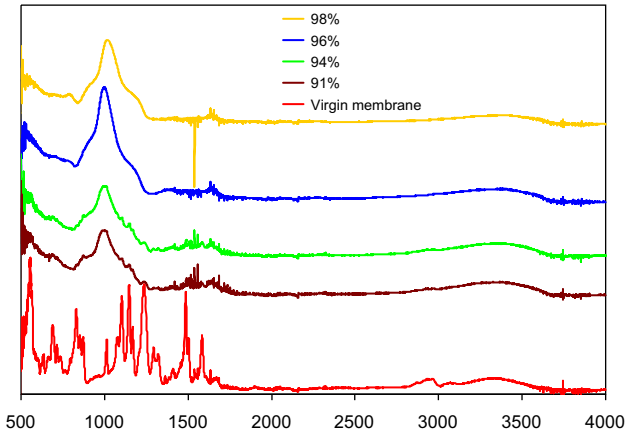

Fig. 4. ATR-FTIR spectra of an RO virgin membrane and the fouled membranes at 91, 94, 96 and 98% recovery.

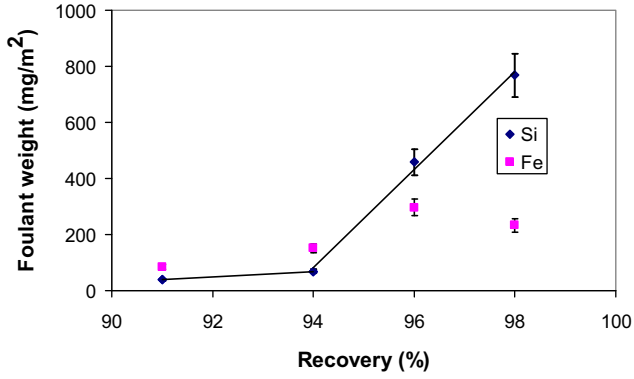

Fig. 5. Foulant weight in the membrane at different recoveries.

some weaker modes between 1,100 and 1,300 cm^{-1} can be seen, which probably belong to the virgin RO membrane.

We also tried to analyze the membrane samples with XRD, but the amount of scaling attached to the membrane was not enough and no peaks could be identified. With Raman spectroscopy, we detected no signal in the membrane samples, so we could not obtain any information from this technique. This may be due to the fact that silica has an extremely weak Raman spectrum [10].

3.1.3. Extraction of silica from the fouled membranes

Small pieces of fouled membrane were soaked in NaOH solution at pH 14 for 3 days and then the solution was analyzed with ICP-MS. The compounds found in the solution were mainly Si and Fe and some traces of K and Al. Although Al is a part of the scaling layer as was determined with EDX [5], Al^{3+} is not soluble at high pH values. Therefore it was only found at trace levels with this method.

Fig. 5 shows the amount of Si and Fe in mg per square meter of membrane found at the four different recoveries. The Fe content seems to increase slowly with the recovery, whereas the Si content shows a slow increase from 91 to 94% recovery and a much faster increase at > 94% recovery.

3.1.4. Concentration polarization

The CP factor for a clean and fouled membrane was calculated for every experiment. We know the average cake layer thickness from observing the cross-section SEM images ([5] and Table 3). Chong [9] found in his research that porosity values for colloidal silica range from 0.6 to 0.4 at zero to 10,000 ppm NaCl, respectively. In our case, we know the total dissolved solids (TDS) in the bulk solution of the feed of the RO, and therefore, we can estimate the porosity **(ε1)** according to these values.

Table 3
CP for a clean and fouled membrane

Recovery (%)	Cp clean membrane	Cake layer average thickness (μm)	TDS (ppm)	TDS equivalent NaCl (ppm)	Estimated Porosity 1 (ε1)	Estimated porosity 2 (ε2)	Average porosity (ε)	Cp fouled membrane
91	1.20	0.5	3,331	2,389	0.55	0.87	0.71	1.20
94	1.18	1	4,768	3,294	0.53	0.88	0.71	1.19
96	1.21	3	7,742	5,273	0.49	0.82	0.66	1.27
98	1.17	5	15,251	10,890	0.38	0.92	0.66	1.25

In addition, from the SEM observations on the thickness of the layer (see Table 3), the weight of Si and Fe found in the dissolution experiments and the estimated densities of the silica and iron (III) oxyhydroxides, one can calculate the volume and weight of scaling and thus obtain an estimate of the effective average porosity **(ε2)** of the fouling layer. However, the fouling layer was only present on about 50% of the membrane surface for the experiments at 91 and 94% recovery. In addition, we observe in the SEM images that the fouling layer shows large empty volumes at recoveries of 94% and higher [5]. This is why the calculated values for porosity are much higher than values reported in the literature for colloidal silica (the majority component of fouling at higher recoveries) of around 0.5 [9]. We have to point out that the experiment at 98% ran for 11 days (the other experiments ran for 3 weeks). Therefore, if it had ran for the same period, we assume we would have had a higher thickness of the fouling layer and also a lower porosity.

In the literature, we also found porosity values for a layer of silica scaling of 0.99 [2]. However, looking at the SEM pictures (Figs. 2 and 3 and [5]) one can see that the fouling layer is quite complex and, for instance, at 96 and 98%, it is possible to differentiate two areas—one compact layer close to the membrane surface and one more open area on the top of it. We estimate a more realistic value of the porosity by averaging the two different estimated porosities.

In the following table, we show the values of CP for a clean and a fouled membrane for different recoveries (Table 3), as calculated with Equation (2).

The CP for a clean membrane is similar to that of the four membranes. However, at 91 and 94 % recovery the CP for a fouled membrane has the same value as for the clean membrane, but at 96 and 98% recovery it is slightly higher.

The silica concentration in the bulk solution of the RO feed was measured by means of ICP-MS and is shown in Fig. 6. These are depicted together with the correction for the CP of clean and fouled membrane and the silica solubility at the experimental conditions (Fig. 6).

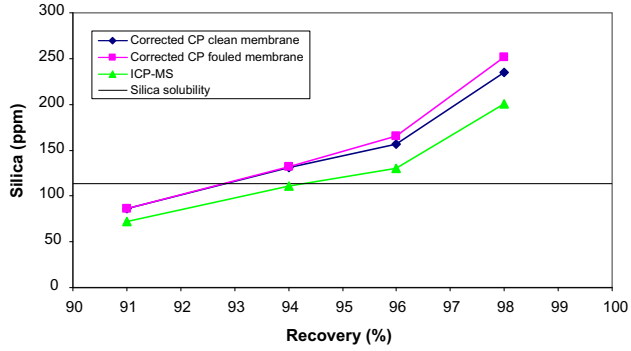

Fig. 6. Silica concentration in the RO feed at different recoveries.

We can see from Fig. 6 that the calculated silica concentration at the membrane surface using CP for a clean and fouled membrane makes a more pronounced difference in the experiments at 96 and 98% recovery. At 91% recovery, the calculated silica concentration at the membrane surface remains below the silica solubility. At 94% recovery, the concentration is slightly above it, and at 96 and 98% the solubility is exceeded. However, the presence of iron and aluminum significantly increases the precipitation of silica, as we showed before [5].

4. Discussion

4.1. Membrane autopsy

From the SEM-EDX analysis, significant differences were observed between the SEM images of the RO membranes obtained at different recoveries. At 96 and 98% recovery, we observed fouling on the membrane from the feed to the concentrate side (not all the images are shown here). The fouling consisted of voluminous amorphous agglomerates. However, at 91 and 94% recovery we observed thin deposits at some areas of the membrane (about 50% coverage).

To characterize the scaling, several techniques were performed. The bulk structures of silica are classified as crystalline and amorphous polymorphs. More than 35 well-defined forms of crystalline silica are known; however, amorphous silica remains poorly characterized. This is due to the lack of sufficiently precise methods to assess the long-range structural order [14].

After trying different techniques to characterize qualitatively the scaling, we only got some results with ATR-FTIR. The four samples from the fouled membranes showed a similar spectrum. The intensity was stronger for the membranes at 96 and 98% recovery due to a higher amount of scaling. All fouled membranes gave a large peak at 1,015 cm^{-1}. This peak could belong to amorphous SiO_2, which normally has a peak at around 1,100 cm^{-1}[10] or amorphous aluminosilicates, which present a strong broad band at 1,032 cm^{-1}, assigned to asymmetric M–O–M stretching (M:Si, Al) [12]. Furthermore the small peak at 800 cm^{-1} is also found in amorphous silica and aluminosilicates [10,12]. In addition, the four membranes showed a broad peak between 3,100 and 3,500 cm^{-1}, which also could be seen in the virgin membrane. However, in the virgin membrane there was also a peak between 2,800 and 3,000 cm^{-1}, but it seemed to disappear or become part of the broad peak between 3,100 and 3,500 cm^{-1} with increasing recovery. This broad band between 2,800 and 3,600 cm^{-1} can be attributed to hydrogen-bond OH surface groups, physisorbed water and other surface species, and also appears in amorphous aluminosilicates, where it is assigned to M–OH stretching. The fact that at 91 and 94% recovery some peaks from the virgin membrane could be seen confirms that the scaling layer at these recoveries was not homogenous along the membrane surface and was thinner.

4.2. Extraction of silica from the membrane

From the experiments to dissolve the scaling, shown in Fig. 5, it can be observed that the amount of Si increased with increasing the recovery. The increase from 91 to 94% is not as high as the increase from 94 to 96%. Therefore, together with the SEM-EDX analysis we can conclude that the Si-scaling increased sharply after 94%, considering it as the scaling threshold for our system and time scale.

The amount of iron in the scaling layer also seemed to increase with the recovery, albeit slowly. The presence of iron confirmed that it plays an important role in silica scaling. As Al^{3+} is not soluble at the high pH used in these experiments, it is not surprising that only trace levels were found. However, Al is also a part of the fouling layer, as was shown elsewhere by SEM-EDX analysis of the fouled membranes [5].

For the estimation of the porosity based on the dissolution experiments, only the Si and Fe were considered. However, there are also other elements present, such as Al and C. Therefore, the average porosity of the scaling layer is most likely lower than the estimated values from the dissolution experiments.

4.3. Concentration polarization

The CP is an important factor to take into account, since it results in a higher local concentration at the membrane surface. The calculation of the CP for a fouled membrane is not an easy task, mainly because it is difficult to obtain reliable porosity values. In this paper, we made several assumptions (see section 3.1.4) to calculate it.

While for a clean membrane the CP has the same value for the four experiments (about 1.2), for a sufficiently fouled membrane there is a difference, giving estimated values of CP of 1.27 and 1.25 at 96 and 98% recovery, respectively. Once the membrane has a significant cake layer, the diffusion of the solutes through the cake is hindered and the concentration of silica near the active layer of the RO membrane increases. This means that the supersaturation of silica is also increased at higher recoveries (see Fig. 6), which in turn leads to faster deposition (scaling) and higher detected levels of Si per m^2 in the dissolution experiments (Fig. 5). The presence of scaling thus enhances the growth speed of the fouling layer.

4.4. General discussion

Previously, we concluded that the layer of fouling found in our system at high recoveries probably consisted of aluminosilicates [5]. Further work has been conducted to confirm this hypothesis. The additional analyses on the fouling layer presented in this paper suggest that whether amorphous silica or amorphous aluminosilicates were the main inorganic component of the fouling layer. In our previous paper, we suggested that the fouling mechanism was a combination of colloidal fouling by either iron (oxy)(hydr)oxides or small colloids with Al, and subsequent growth of aluminosilicates on these colloids. Looking at the observations and data provided in this paper, we could confirm this. Furthermore, we postulated that aluminosilicate scaling took of above 94% recovery, which can be explained with Fig. 6 where it can be seen that

from 94% recovery on we have sufficient silica supersaturation.

5. Conclusions

In our system, the limiting recovery to prevent problematic scaling in the RO membrane is about 94% based on the experiments for our time scale. To operate the system at recoveries above 94%, the silica must be either removed prior to RO treatment or kept in solution during RO treatment [5]. Here we show the following:

- The SEM-EDX analyses can be used to determine the amount, structure and composition of the scaling layer qualitatively.
- The ATR-FTIR analyses suggested that the main compound in the scaling layer could be either amorphous silica or amorphous aluminosilicates.
- The extraction of silica from the fouled membranes can be used to determine the amount of Si and Fe in the membrane. The amount of Fe only slowly increases with recovery, but the amount of Si increases very quickly above 94% recovery, indicating the onset of (alumino)silicate scaling.
- CP is an important factor that greatly enhances the silica concentration at the active layer of the membrane and leads to enhanced scaling.

Acknowledgements

This work was performed in the TTIW-cooperation framework of Wetsus, Centre of Excellence for Sustainable Water Technology (www.wetsus.nl). Wetsus is funded by the Dutch Ministry of Economic Affairs, the European Union Regional Development Fund, the Province of Fryslân, the City of Leeuwarden and the EZ/Kompas program of the "Samenwerkingsverband Noord-Nederland" and by the Joint Research Programme of the Dutch Water Companies. The authors like to thank the participants of the research theme "Clean Water Technology" for the discussions and their financial support. They would specially like to thank Hans Huiting for the fruitful discussions about this project and Kamuran Yasadi for the ATR-FTIR analysis.

References

[1] R. Sheikholeslami, S. Tan, Effects of water quality on silica fouling of desalination plants, Desalination 126(1–3) (1999) 267–280.
[2] R. Semiat, I. Sutzkover, D. Hasson, Scaling of RO membranes from silica supersaturated solutions, Desalination 157(1–3) (2003) 169–191.
[3] M. Badruzzaman, A. Subramani, J. DeCarolis, W. Pearce, J.G. Jacangelo, Impacts of silica on the sustainable productivity of reverse osmosis membranes treating low-salinity brackish groundwater, Desalination 279(1–3) (2011) 210–218.
[4] R.K. Iler, The Chemistry of Silica; Solubility, Polymerization, Colloid and Surface Properties, and Biochemistry, John Wiley & Sons, New York, NY, 866 1979.
[5] S. Salvador Cob, C. Beaupin, B. Hofs, M.M. Nederlof, D.J.H. Harmsen, E.R. Cornelissen, A. Zwijnenburg, F.E. Genceli Guner, G.J. Witkamp, Silica and silica-derived precipitants as limiting factor in high-recovery reverse osmosis operations. submitted, 2012.
[6] P.M. Dove, N. Han, J.J. De Yoreo, Mechanisms of classical crystal growth theory explain quartz and silicate dissolution behavior, Proc. Nat. Acad. Sci. U.S.A 102(43) (2005) 15357–15362.
[7] P.M. Dove, N. Han, A.F. Wallace, J.J. De Yoreo, Kinetics of amorphous silica dissolution and the paradox of the silica polymorphs, Proc. Nat. Acad. Sci. U.S.A 105(29) (2008) 9903–9908.
[8] M. Mulder, Basic Principles of Membrane Technology, Second ed., Kluwer, Dordrecht, 1996.
[9] T.H. Chong, F.S. Wong, A.G. Fane, Implications of critical flux and cake enhanced osmotic pressure (CEOP) on colloidal fouling in reverse osmosis: Experimental observations, J. Membr. Sci. 314(1–2) (2008) 101–111.
[10] K.D.O. Jackson, A guide to identifying common inorganic fillers and activators using vibrational spectroscopy, Internet J. Vib. Spectro. 2 (2004).
[11] S.B. Howerton, C. Lee, V.L. McGuffin, Additivity of statistical moments in the exponentially modified Gaussian model of chromatography, Anal. Chim. Acta 478(1) (2003) PII S0003–2670(02)01472-1.
[12] O. Martínez-Zapata, J. Méndez-Vivar, P. Bosch, V.H. Lara, Synthesis and characterization of amorphous aluminosilicates prepared by sol–gel to encapsulate organic dyes, J. Non-Crys. Solids 357(19–20) (2011) 3480–3485.
[13] M.S. Seehra, P. Roy, A. Raman, A. Manivannan, Structural investigations of synthetic ferrihydrite nanoparticles doped with Si, Solid State Commun. 130(9) (2004) 597–601.
[14] H.E. Bergna, W.O. Roberts, Colloidal Silica Fundamentals and Applications, Taylor & Francis, Boca Raton, FL, 2006.